BIOCHEMISTRY
including biophysical chemistry & molecular biology

Article

pubs.acs.org/biochemistry

Tryptophan-Dependent Membrane Interaction and Heteromerization with the Internal Fusion Peptide by the Membrane Proximal External Region of SARS-CoV Spike Protein

Ying Liao,[†,‡] Si Min Zhang,[†,§] Tuan Ling Neo,[†] and James P. Tam*[,†]

[†]School of Biological Sciences, Nanyang Technological University, 60 Nanyang Drive, Singapore 637551

[‡]Shanghai Veterinary Research Institute, Chinese Academy of Agricultural Sciences, Shanghai, China

[§]Division of Clinical Microbiology, Department of Laboratory Medicine, Karolinska Institutet, SE-141 86 Stockholm, Sweden

ABSTRACT: The spike (S) protein of severe acute respiratory syndrome-associated CoV (SARS-CoV) mediates membrane fusion and viral entry. These events involve structural rearrangements, including heteromerization between two heptad repeats (HR1 and HR2) to form a trimer of dimers as a six-helix bundle (6-HB), a quaternary protein structure that brings two distant clusters of hydrophobic sequences into the proximity of each other, the internal fusion peptide (IFP) preceding HR1, and the highly conserved tryptophan (Trp)-rich membrane proximal external region (MPER) following HR2. Here, we show that MPER can undergo self-oligomerization and heteromerization with IFP, events that are Trp-dependent. To delineate the roles of Trp residues of MPER in forming these quaternary structures and interacting with membranes, we employed a panel of synthetic peptides: MPER peptide (M-wt) and its alanine (Ala) and phenylalanine (Phe) analogues. Ala substitutions of Trp inhibited its association with cellular membranes. Chemical cross-linking experiments showed that M-wt can self-interact to form oligomers and cross-interact with IFP23, a synthetic IFP peptide, to form a heterohexamer. In comparison, little high-order oligomer was formed between M-wt and fusion peptide. The specific interaction between M-wt and IFP23 was confirmed by immunofluorescence staining experiments. In aqueous solutions, both M-wt and IFP23 displayed random secondary structures that became helical in hydrophobic solvents. Triple-Ala substitutions of Trp in M-wt, but not the corresponding triple-Phe analogue, disrupted oligomerization of M-wt and hetero-oligomerization of M-wt with IFP23. Overall, our results show that Trp residues of MPER play a key role in maintaining the structure and functions of MPER, allowing it to interact with IFP to form a MPER−IFP heteromer, a putative quaternary structure extending from the 6-HB, and function in membrane fusion. Finally, we showed that a MPER peptide could serve as an inhibitor in the entry process.

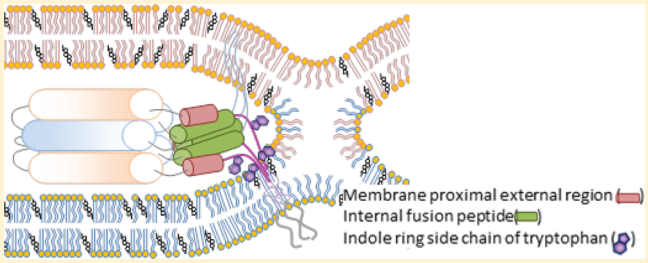

Severe acute respiratory syndrome (SARS) is a contagious atypical pneumonia that caused an epidemic between November 2002 and July 2003 with a 9.6% mortality rate. A previously uncharacterized virus, SARS-associated coronavirus (SARS-CoV), was isolated from patients as the causative agent.[1,2] The SARS-CoV genome contains a characteristic gene order of 5′-replicase, spike, envelope, membrane, nucleocapsid-3′, and short untranslated regions at both termini.[3]

The spike (S) protein, a noncovalently associated trimer, is a stable quaternary protein structure protruding from the virion surface of coronavirus. It is responsible for viral attachment, fusion, and entry into host cells. In SARS-CoV, the S protein becomes fusion competent as it is cleaved into S1 and S2 subunits at amino acid 679 by cathepsin L.[4,5] The S1 subunit mediates receptor binding and determines tropism,[6] whereas the S2 subunit mediates fusion of viral and cellular membranes.[7,8] Two fusion peptides, FP (fusion peptide) comprising amino acids (aa) 770−778 and IFP (internal fusion peptide) comprising aa 856−888, are located at the N-terminus of the S2 subunit, upstream from heptad repeat 1 (HR1) and heptad repeat 2 (HR2).[9−12] In the prefusion state, these fusion peptides are buried in the S protein. Upon receptor binding and cleavage, conformational changes in the S1 subunit and the dissociation of the S1 subunit from the S2 subunit are thought to initiate two major rearrangements in the S2 trimer. First, FP is exposed and then inserted into the target cell membrane, connecting the virus and the target cell. Second, HR2 folds back onto HR1 through a complementary interaction between aa 916−950 of HR1 and aa 1151−1185 of HR2,[8] resulting in an antiparallel six-helix bundle (6-HB).[7,13,14] In turn, it facilitates the apposition of virus and target cell membranes to sufficient proximity, allowing the mixing and fusion of lipid bilayers, leading to virus entry.

The formation of a 6-HB is characteristic of a class I fusion protein, and the best understood peptide−peptide interaction through helices in forming quaternary protein structures to facilitate the fusion process. Subsequent events following the

Received: October 30, 2014
Revised: January 16, 2015
Published: February 10, 2015

DOI: 10.1021/bi501352u
Biochemistry 2015, 54, 1819−1830

Table 1. Sequential Alignment of the S Protein MPER from Members of Coronaviride

group I	HCoV-229E	Y	I	K	**W**	P	**W**	W	V	**W**	L
	PEDV	Y	I	K	**W**	P	**W**	W	V	**W**	L
	HCoV-NL63	Y	I	K	**W**	P	**W**	W	V	**W**	L
	TGEV	Y	V	K	**W**	P	**W**	Y	V	**W**	L
	FCoV	Y	V	K	**W**	P	**W**	Y	V	**W**	L
	FIPV	Y	V	K	**W**	P	**W**	Y	V	**W**	L
	PRCoV	Y	V	K	**W**	P	**W**	Y	V	**W**	L
	CCoV	Y	V	K	**W**	P	**W**	Y	V	**W**	L
group II	MHV	Y	V	K	**W**	P	**W**	Y	V	**W**	L
	HCoV-OC43	Y	V	K	**W**	P	**W**	Y	V	**W**	L
	BCoV	Y	V	K	**W**	P	**W**	Y	V	**W**	L
	RCoV	Y	V	K	**W**	P	**W**	Y	V	**W**	L
	HEV	Y	V	K	**W**	P	**W**	Y	V	**W**	L
	SDAV	Y	V	K	**W**	P	**W**	Y	V	**W**	L
	HKU1	Y	V	K	**W**	P	**W**	Y	V	**W**	L
	CRCoV	Y	V	K	**W**	P	**W**	Y	V	**W**	L
	ECoV	Y	V	K	**W**	P	**W**	Y	V	**W**	L
	MERS-CoV	Y	N	K	**W**	P	**W**	Y	V	**W**	L
	SARS-CoV	Y	I	K	**W**	P	**W**	Y	V	**W**	L
	Bat-SARS-CoV	Y	I	K	**W**	P	**W**	Y	V	**W**	L
group III	IBV	Y	I	K	**W**	P	**W**	Y	V	**W**	L
	TCoV	Y	I	K	**W**	P	**W**	Y	V	**W**	L
	PCoV	Y	I	K	**W**	P	**W**	Y	V	**W**	L
	DCoV	Y	I	K	**W**	P	**W**	Y	V	**W**	L

formation of the 6-HB contributing to membrane fusion remain to be elucidated in detail.

The FP located at the N-terminus of the S2 protein is known to be responsible for cell membrane insertion.[9] In contrast, the role of IFP, a hydrophobic segment following FP, is poorly understood. Mutations in IFP have been shown to inhibit 70% of the S protein-mediated cell fusion,[15] but the mechanism of such an inhibition has not been clearly defined. In addition to FP and IFP, the SARS-CoV S protein contains a third hydrophobic and membrane-active region, the membrane proximal external region (MPER).[9−12,16,17] The MPER, Y(V/I)KWPW(W/Y)VWL, located between HR2 and the transmembrane (TM) domain of the S2 protein, is rich in aromatic amino acid residues with three or four Trp (W) and two or three Tyr (Y) residues (Table 1). All coronavirus S proteins share a highly conserved MPER,[18−20] and such sequence conservation is also found in other viruses with class I fusion protein, such as human immunodeficiency virus type 1 (HIV-1),[21] feline immunodeficiency virus (FIV),[22] influenza virus,[23] and Ebola virus.[24]

Previously, we have reported that Trp residues in the MPER are essential for effective viral infection through a mutational study.[19] Single or multiple Ala substitutions of Trp residues in the SARS-CoV MPER abrogate the viral infection, whereas replacing the Trp residues with an aromatic amino acid such as Phe partially restores the infectivity. Biophysical studies suggested that the MPER facilitates viral infection by perturbing lipid bilayers and inducing lipid mixing through peptide−lipid interaction.[18−20,25] Synthetic peptides derived from the SARS-CoV S protein MPER strongly partitioned into the liposomal membranes, perturbed the membrane, and caused content leakage.[10,11,17] Similar studies of HIV-1 envelope protein and Ebola virus GP2 using MPER-derived peptides reached similar conclusions, supporting the ability of MPER to interact with lipid membranes.[24,26] Furthermore, the MPER has been proposed to be structurally flexible. Synthetic MPER peptides derived from HIV envelope protein, Ebola virus GP2, and influenza virus HA protein have been shown to undergo secondary structural changes that include transitions from a predominant β-strand to an α-helix at different pHs or when in contact with lipid membranes.[21,23,27,28] The structural plasticity of the MPER together with our mutational study showing the important role played by the Trp residues in viral infectivity raises the possibility that the MPER may have an additional partner of interaction, apart from the lipid membranes, in the fusion process. A potential interaction partner of the MPER is the IFP, which is placed on the same side of the 6-HB and in the proximity of the MPER. A putative MPER−IFP complex through a peptide−peptide interaction would provide a quaternary structure that could facilitate the membrane fusion process.

Here we describe a structure−activity relationship study of the MPER using a panel of synthetic peptides to define the roles played by its Trp residues in forming a putative new quaternary structure of the MPER−IFP complex in the virus−membrane fusion process. Our results show the oligomerization of the MPER and the peptide−peptide interaction with IFP through self-complementary and complementary interactions, respectively, and these interactions are Trp-dependent. The Trp residues, particularly Trp1194, played important roles in maintaining the structural plasticity of the MPER and in allowing peptide−lipid interaction with the cellular membrane. Thus, the MPER−IFP complex may contribute to a quaternary protein structure serving as an extension to the 6-HB to facilitate the fusion of viral and host cell membranes. Lastly, we show that MPER-derived peptides displayed a fusion inhibitory effect against viral entry.

EXPERIMENTAL PROCEDURES

Solid Phase Peptide Synthesis. All amino acids and coupling reagents were purchased from Novabiochem (San Diego, CA). Peptides were synthesized using the microwave

DOI: 10.1021/bi501352u
Biochemistry 2015, 54, 1819−1830

peptide synthesizer by 9-fluorenylmethoxycarbonyl (Fmoc) chemistry according to the manufacturer's instructions. Non-biotinylated peptides were synthesized with Wang resin, and C-terminally biotinylated peptides were synthesized with Fmoc-Lys(biotin)-Rink amide resin. Briefly, 0.1 mmol of resin (0.2 mmol/g) (Louiswille, KY) was swolen in 5 mL of dichloromethane (DCM) and subsequently in 10 mL of dimethylformamide (DMF). For each coupling, Fmoc was removed by 20% piperidine in DMF, followed by the addition of 0.5 mmol of the Fmoc-protected amino acid. For hindered amino acids such as Fmoc-Arg(Pbf) and Fmoc-Pro, a double-coupling procedure was performed. The Fmoc-protected amino acid was activated by pyBop (26 g/100 mL of DMF) and diisopropylethylamine (DIEA, 35 mL in 65 mL of DMF). The coupling was performed under microwave conditions. The final removal of side-chain protection groups and the cleavage of the peptide from the resin were performed with 10 mL of reagent R [90% trifluoroacetic acid (TFA), 5% thioanisole, 3% ethylene thiol, and 2% anisole] with agitation for 3 h. Resin was removed by filtration, and the peptide in TFA was precipitated with 100 mL of diethyl ether via centrifugation at 4000 rpm and 4 °C for 10 min. The peptide was washed three times in diethyl ether. All peptides were purified by high-performance liquid chromatography (HPLC), and their molecular masses were confirmed by matrix-assisted laser desorption ionization time-of-flight mass spectrometry.

Circular Dichroism (CD) Spectroscopy. CD spectroscopy analysis was performed to study the secondary structure of a single peptide or a combination of two peptides (M-wt/IFP23) in increasing trifluoroethanol (TFE) concentrations. TFE was used as a lipid mimetic. The induced environmental changes mimic the increase in local environmental hydrophobicity as experienced by membrane proximal sequences during the later stages of membrane fusion.[29] Peptide (1 mM) dissolved in water with increasing TFE concentrations was subjected to CD spectroscopy using a Chirascan CD spectrometer (Applied Photophysics). Cells with a 0.1 mm path length (Hellma UK Ltd.) were used for all the measurements at 25 °C. Samples were measured between 190 and 240 nm, with a 0.1 nm step resolution, a measurement speed of 60 nm/min, and a 1 nm bandwidth. Baselines were either water or the respective buffer solutions in which the peptides were dissolved. At least four repeat scans were obtained for each sample and its respective baseline. The average baseline spectrum was subtracted from the average sample spectrum before the net spectrum was smoothed with a Savitsky−Golay filter. Secondary structure analyses were performed using CDNN with the respective spectrum as input. The secondary structure contents were then plotted against the TFE percentage used in the experiments.

Chemical Cross-Linking, Tricine Sodium Dodecyl Sulfate Polyacrylamide Gel Electrophoresis (SDS−PAGE), Silver Staining, and Western Blot Analysis. Peptide (1 mM) was incubated with 0, 1, or 5 mM glutaraldehyde at room temperature for 1 h and subjected to Tricine SDS−PAGE and silver staining or Western blotting. Tricine SDS−PAGE was performed as previously described.[30] For silver staining, gels were first fixed in fixing buffer (50% methanol, 10% acetic acid, and 100 mM ammonium acetate) for 30 min and then washed twice with H_2O (doubly distilled) for 30 min each. Gels were then sensitized in 0.005% sodium thiosulfate for 30 min, before being stained with 0.1% silver nitrate for 30 min. After being washed with H_2O, gels were incubated in developer (0.036% formaldehyde and 2% sodium carbonate), and the development process was stopped by incubating the gel in 50 mM EDTA for 30 min. Western blotting was conducted using Avidin-HRP (Cell Signaling). Membranes were developed with an enhanced chemiluminescence (ECL) detection system (Amersham Pharmacia) and exposed to X-ray film (Fuji). All procedures were performed at room temperature.

Immunofluorescence Assay. Vero E6 cells were seeded on four-well chamber slides at 50% confluence 1 day prior to the experiment; 50 μM peptides were applied to the cells and the cells incubated at 37 °C for 30 min. Peptides were then removed, and the cells were washed thrice in PBS (phosphate-buffered saline). The cells were then incubated for 30 min at 4 °C with both Alexa Fluor 594-conjugated CT-B (10 μg/mL) and DylightTM 488-conjugated NeutravidinTM [1:200 (v/v) in PBS supplemented with 0.1% BSA (bovine serum albumin)]. Subsequently, the cells were incubated with rabbit anti-CT-B antibody [1:50 (v/v), 30 min, 4 °C], which would initiate raft aggregation, making rafts visible as patches under a confocal microscope. The cells were subsequently permeabilized with 0.2% Triton X-100 in PBS for 10 min and incubated with 0.1 μg/mL DAPI in PBS for 10 min in the dark. The cells were fixed with 4% paraformaldehyde (15 min, 4 °C). The specimens were mounted with glass coverslips using fluorescent mounting medium containing 15 mM NaN_3. The cells were washed thrice in PBS between incubations. Fluorescently labeled cells were analyzed with a Zeiss LSM 510 META laser scanning confocal microscope with 40× objective lenses. The images were processed using LSM 510 META software.

Biochemical Isolation of Lipid Rafts. Cells ($2-5 \times 10^7$) were washed thrice with ice-cold PBS and lysed on ice for 30 min in 1 mL of 1% Triton X-100 TNE lysis buffer supplemented with complete protease inhibitor cocktail. The cell lysates were centrifuged for 5 min (4000*g* and 4 °C) to remove cell debris and nuclei. The supernatant was mixed with 1 mL of TNE buffer with 80% sucrose, placed at the bottom of the ultracentrifuge tube, and overlaid with 6 mL of 30% and 3 mL of 5% sucrose in TNE buffer. The lysates were ultracentrifuged at 4 °C in an SW41 rotor (Beckman) for 18 h at 38000 rpm. After centrifugation, 11 fractions (1 mL each) were collected from the top to the bottom of the tube and subjected to 16% Tricine SDS−PAGE or 10% glycine SDS−PAGE, followed by Western blotting using Avidin-HRP, anti-S antibody, or anti-caveolin-1 antibody.

IBV-Luc Preparation. The egg-adapted Beaudette strain of avian infectious bronchitis virus (IBV) (ATCC VR-22) adapted to Vero E6 cells was used in this study. IBV-Luc was constructed by replacing the 3a3b ORF with the firefly luciferase gene using an *in vitro* ligation protocol. The virus was recovered from Vero E6 cells electroporated with *in vitro* transcripts generated from the full-length IBV-Luc cDNA. Virus stocks were prepared from the infection of Vero cells with 0.1 PFU of virus per cell and incubation at 37 °C for 24 h. After three rounds of freeze and thaw cycles, cell lysates were spun down at 3000 rpm. Aliquots of the supernatants were stored at −80 °C as virus stock. Virus titers were determined by a plaque assay with Vero cells; 1 PFU of virus per cell was used to infect cells in experiment. Vero E6 cells were maintained in Dulbecco's modified Eagle's medium (DMEM) supplemented with 10% fetal bovine serum and grown at 37 °C in 5% CO_2.

Virus Inhibition Assay and PrestoBlue Cell Viability Assay on Vero E6 Cells. Vero E6 cells were seeded in the 96-well plates 1 day before infection. Different concentrations of

DOI: 10.1021/bi501352u
Biochemistry 2015, 54, 1819−1830

Table 2. Design and Sequences of Synthetic Peptides Derived from CoV S Protein

designation	virus	region (amino acid positions)	sequence
M-wt	SARS-CoV	MPER (1187−1202)	KYEQYIKWPWYVWLGF
M-W1194A	SARS-CoV	MPER (1187−1202)	KYEQYIKAPWYVWLGF
M-W1196A	SARS-CoV	MPER (1187−1202)	KYEQYIKWPAYVWLGF
M-Y1197A	SARS-CoV	MPER (1187−1202)	KYEQYIKWPWAVWLGF
M-W1199A	SARS-CoV	MPER (1187−1202)	KYEQYIKWPWYVALGF
M-F1202A	SARS-CoV	MPER (1187−1202)	KYEQYIKWPWYVWLGA
M-3W3A	SARS-CoV	MPER (1187−1202)	KYEQYIKAPAYVALGF
M-3W3F	SARS-CoV	MPER (1187−1202)	KYEQYIKFPFYVFLGF
M-ibv	IBV	MPER (1186−1202)	LKTYIKWPWYVWLAIAF
FP19	SARS-CoV	FP (770−788)	MYKTPTLKYFGGFNFSQIL
IFP23	SARS-CoV	IFP (866−888)	AGWTFGAGAALQIPFAMQMAYRF
TE20	SARS-CoV	aa 743−762	TQLNRALSGIAAEQDRNTRE

peptides were dissolved in serum free DMEM. IBV-Luc was incubated with peptides for 1 h at 37 °C, prior to being added to the cells at 1 PFU. Virus and peptides were removed 1 h postinfection. The cells were incubated for an additional 20 h and subsequently subjected to a luciferase assay according to the manufacturer's instructions (Promega). Briefly, upon removal of medium, the cells were rinsed in PBS, lysed with 20 μL of lysis buffer per well, and assayed with 100 μL of luciferase assay reagent per well. The percentage of infectivity was determined by luciferase activity.

The cytotoxicity effects of the peptides on Vero E6 cells were determined by a PrestoBlue cell viability assay (Invitrogen), according to the manufacturer's protocol. Briefly, peptides at different concentrations were added to Vero E6 cells seeded in 96-well plates. After incubation for 20 h, PrestoBlue cell viability reagent was added to cells, and the cells were incubated for 10 min at 37 °C. The resulting fluorescence signal was then read and recorded.

RESULTS

Design and Synthesis of FP, IFP, MPER Peptides, and Their Ala or Phe Analogues. To provide mechanistic insight into our previous work using pseudotyped SARS-CoV showing that mutating Trp to Ala or Phe in the S protein MPER abrogated or diminished infectivity, respectively,[19] we designed a panel of synthetic peptides derived from the MPER, FP, and IFP, all of which were synthesized by solid phase peptide synthesis (Table 2). The highly hydrophobic nature of the MPER peptide necessitated the inclusion of the upstream charged residues (KYEQ) in the MPER peptide as M-wt (KYEQYIKWPWYVWLGF) to increase its aqueous solubility and to facilitate its purification by reverse phase HPLC. The Trp, Tyr, or Phe residues (W1194, W1196, Y1197, and W1199) in the M-wt analogues, M-W1194A, M-W1196A, M-Y1197A, M-W1199A, M-F1202A, M-3W3A, and M-3W3F, and F1202 were substituted with Ala or Phe individually or in combination. Synthetic peptides FP19, IFP23, and TE20 (see Table 2 for their sequences) were derived from FP,[16] IFP,[10,11] and the region upstream from FP (aa 743−762), respectively. To facilitate product detection in chemical crossing experiments, all peptides were also synthesized with a C-terminal biotin tag and are designated with the letter b following their names (e.g., M-wtb). M-ibv was derived from the MPER of another CoV, avian infectious bronchitis virus (IBV), and designed specifically for the virus neutralization study.

Interaction of MPER Peptides with Biological Membranes and the Role of Their Trp Residues. To examine the interaction between MPER-derived peptides and the biological membrane in detail, we employed a live cell system using Vero E6 cells, which are susceptible to SARS-CoV infection. In these experiments, MPER and its analogues were tagged with biotin. They included M-wtb, M-3W3Ab, and a triple-Phe MPER analogue, M-3W3Fb, with all three Trp residues in the MPER replaced with Phe.

First, to study the cellular retention of MPER-derived peptides when they are applied exogenously, M-wtb, M-3W3Ab, and M-3W3Fb were incubated with Vero E6 cells for 1 h. Cells and medium were harvested, and the retained peptides were detected by immunoblots using avidin-HRP. M-wtb and M-3W3Fb were readily detectable in cell lysate, suggesting cellular retention. Meanwhile, triple-Ala substitutions of M-wtb abrogated the effect (Figure 1). This suggest an important role of aromatic side chains in the association between the MPER and the cellular membrane.

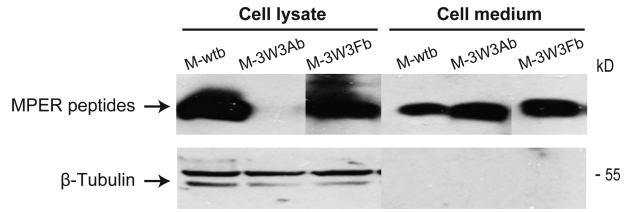

Figure 1. Cell binding ability of M-wt and its Ala substitution analogues. M-wtb, M-3W3Ab, or M-3W3Fb (50 μM each) was incubated with Vero E6 cells for 30 min. Cells and medium were harvested and subjected to 16% Tricine SDS−PAGE and Western blotting using Avidin-HRP.

Immunofluorescence staining was then used to determine the location of the retained MPER peptides. Positive signals were detected in Vero E6 cells treated with M-wtb and M-3W3Fb (Figure 2A). Their signals partially colocalized with that of GM1, a lipid raft marker. In agreement with the cell retention experiment, there was no detectable peptide signal in the M-3W3Ab-treated cells.

Taken together, these results confirmed that the MPER-derived peptide bound to biological membranes, and that its aromatic residues are essential for the MPER−membrane interaction.

The immunofluorescence staining showed that M-wtb partially colocalized with the lipid raft marker GM1. The N-terminal region of the SARS-CoV MPER, specifically, 1187 KYEQYIK 1193, shares sequential homology with the cholesterol recognition amino acid consensus motif, L/V-

DOI: 10.1021/bi501352u
Biochemistry 2015, 54, 1819−1830

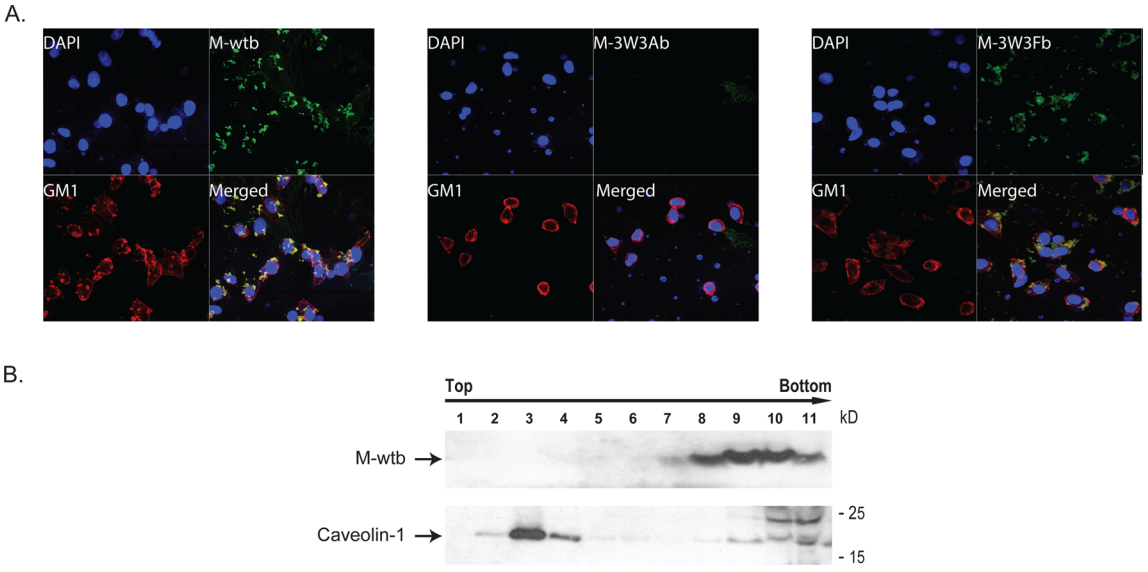

Figure 2. Cell membrane binding by MPER peptides and the role of Trp residues. (A) Membrane binding of M-wt and its analogues. Vero E6 cells were treated with 50 μM M-wt-b, M-3W3Ab, or M-3W3Fb for 30 min and subjected to immunofluorescence staining with Alex Fluor 594-conjugated CT-B (lipid raft marker GM1 staining, red), Dylight 488-conjugated Neutravidin (biotin staining, green), and DAPI (nucleus staining, purple). M-wt attached to the cells, while its triple-Ala-substituted analogue, M-3W3A, lost the membrane interaction ability. Triple-Phe substitution of M-wt partially rescued the phenotype. (B) Exogenously applied M-wt_b did not show preferential location to lipid rafts. Vero E6 cells were pretreated with 50 μM M-wtb for 30 min and lysed on ice in 1% Triton X-100 TNE lysis buffer. Lipid raft fractions were then isolated from postnuclear cell extracts through a membrane flotation assay. Eleven fractions were collected from top to bottom after centrifugation and subjected to 16% Tricine SDS−PAGE (for detection of M-wtb) and 10% glycine SDS−PAGE (for detection of caveolin-1). Western blotting was performed using Avidin-HRP or anti-caveolin-1 antibody.

X(1−5)-Y-X(1−5)-R/K, in which X(1−5) represents one to five residues of any amino acid.[31] The motif was believed to result in a peptide or protein that preferentially associates with cholesterol, a principal component of lipid rafts.

We next examined if the exogenously applied M-wtb was preferentially recruited onto plasma membrane lipid rafts. Lipid rafts were isolated successfully via a membrane flotation assay, as highlighted by the raft-associated protein caveolin-1 in fractions 2−4 (Figure 2B). Surprisingly, exogenously applied MPER peptide did not cofractionate with caveolin-1 in fractions 2−4 but was detected in fractions 7−11. These results suggest two possibilities. First, lipid rafts and their associated proteins are not high-affinity binding targets for the exogenously applied peptide M-wtb, which is a monomer. Second, the association requires that the MPER be in a quaternary structure complex, as either an oligomer or a hetero-oligomer with another domain in the S protein. The second possibility is investigated below.

MPER−MPER Interaction and the Role of Trp. The SARS-CoV S protein interacts through multiple domains, including self-binding of HR1 and HR2 in the prefusion state as a trimer and complementary binding of HR1 and HR2 to form the 6-HB as a trimer of dimers in the fusion state. As the MPER is the region following HR2, we next investigated the interaction of the SARS-CoV MPER to form a quaternary structure similar to that of HR2, and the role of Trp residues in this process. Synthetic MPER peptides were studied by *in vitro* chemical cross-linking experiments, and glutaraldehyde was used as a cross-linker to stabilize transient and weak noncovalent interactions through covalent bonds. Without glutaraldehyde, M-wt produced a single band with a molecular weight corresponding to that of the monomer (2200 Da), as SDS dissociates the noncovalently associated oligomers (Figure 3). With glutaraldehyde, the M-wt peptide produced dimer,

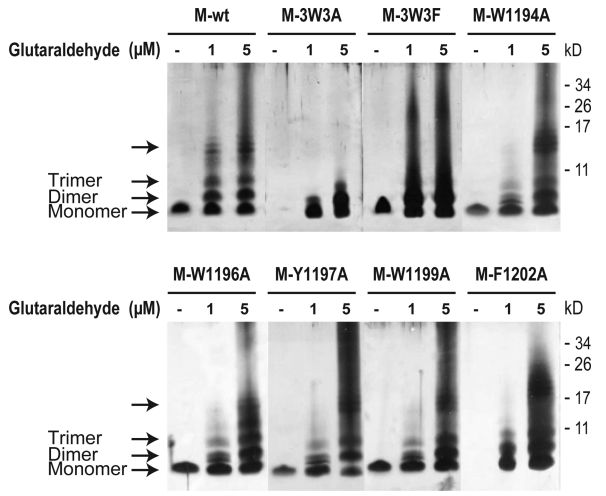

Figure 3. Importance of Trp residues in self-interaction of MPER peptides. M-wt, M-3W3A, M-3W3F, M-W1194A, M-W1196A, M-Y1197A, M-W1199A, or M-F1202A (1 mM each) was incubated with 0, 1, or 5 mM glutaraldehyde at room temperature for 1 h. Samples were subjected to 16% Tricine SDS−PAGE and silver staining.

trimer, and high-molecular weight oligomers, suggesting that the MPER sequence possesses a self-interaction potential. The putative oligomer is termed MPER−MPER interaction hereafter. The level of oligomeric formation in M-wt increased with an increasing glutaraldehyde concentration. Similarly, high-molecular weight oligomers were observed for the single-Ala substitution analogues M-W1194A, M-W1196A, M-Y1197A, M-W1199A, and M-F1202A. However, no trimer or high-order oligomers were detected in the triple-Ala analogue M-3W3A after cross-linking by glutaraldehyde. M-3W3F rescued this self-binding ability to form oligomers, suggesting that aromatic side

DOI: 10.1021/bi501352u
Biochemistry 2015, 54, 1819−1830

chains are essential for MPER−MPER interaction. However, instead of a discrete order of oligomers, M-3W3F formed a continuous band of oligomers, suggesting an altered MPER−MPER interaction pattern upon triple Trp → Phe mutation.

MPER−IFP Heterohexamer Formation and the Role of Trp in MPER−IFP Interaction. After the receptor binds to initiate the insertion of N-terminal FP (aa 770−788) into the membrane and HR1 and HR2 form the 6-HB,[9,16] FP and IFP (aa 858−886) are positioned adjacent to the MPER. We envisioned that their proximity may facilitate heteromerization between the N-terminal hydrophobic sequences of IFP and MPER. This hypothesis was investigated by *in vitro* chemical cross-linking of FP- and IFP-derived peptides, FP19 and IFP29, respectively, with MPER-derived peptides. Peptide TE20 (aa 743−762) was used as a negative control. FP19, IFP23, and TE20 were synthesized with a biotin tag at their C-termini to facilitate detection by Western blot and are designated FP19b, IFP29b, and TE20b, respectively. Any signal detected by avidin-HRP in the Western blots represented FP19b, IFP23b, or TE20b, but not nonbiotinylated MPER peptides. Without MPER peptides, FP19b and IFP23b formed mainly dimers with increasing concentrations of glutaraldehyde (Figure 4A), suggesting that the highly hydrophobic FP and IFP sequences could self-interact. TE20 failed to oligomerize even in 2.5 mM glutaraldehyde (Figure 4A). When M-wt was mixed with IFP23b, a predominant heterotrimer was observed at 1 mM glutaraldehyde. At 2.5 mM glutaraldehyde, heterotrimers, heterotetramers, and heterohexamers were observed (Figure 4A). However, FP19b and TE20b produced few high-order hetero-oligomers upon being mixed with M-wt. Taken together, these results suggest the MPER and IFP contain sequence specificity for complementary interactions, leading to the formation of heterohexamers. In contrast, such interaction was not observed between the MPER and the other N-terminal hydrophobic region, FP.

To investigate the influence of Trp → Ala and Trp → Phe substitutions on the putative MPER−IFP interaction, M-3W3A and M-3W3F were separately cross-linked with IFP23b, FP19b, or TE20b. As shown in Figure 4B, no oligomer was observed in the IFP23b/M-3W3A, FP19b/M-3W3A, or TE20b/M-3W3A mixture, indicating that M-3W3A could not produce high-order oligomers with the FP19b, IFP23b, or TE20b peptide. Oligomers were observed in the IFP23b/M-3W3F mixture at 2.5 mM glutaraldehyde. However, they produced bands weaker than those observed for the IFP23b/M-wt mixture. FP19b and TE20b peptides remained in monomeric form in the presence of M-3W3F. These results demonstrate that Trp residues in the MPER are important for MPER−IFP interaction. The Trp indole ring may play a role in maintaining the specific interaction between the MPER and IFP, as it cannot be fully replaced by the phenyl side chain of Phe.

In the previous section, we showed that the exogenously applied M-wtb was partially recruited onto plasma membrane lipid rafts through immunofluorescence staining. We next asked whether MPER- and IFP-derived peptides could form non-covalent complexes upon being exogenously applied to Vero E6 cells, under a physiologically relevant condition, to facilitate the recruitment of IFP-derived peptides to the cell membrane. IFP23b was applied to cells alone or in combination with M-wt, M-3W3A, or M-3W3F. The signal detected by immunofluorescence staining using Dylight 488-conjugated Neutravidin represents IFP23b. When cells were incubated with IFP23b alone, only small amounts of peptides were detected and

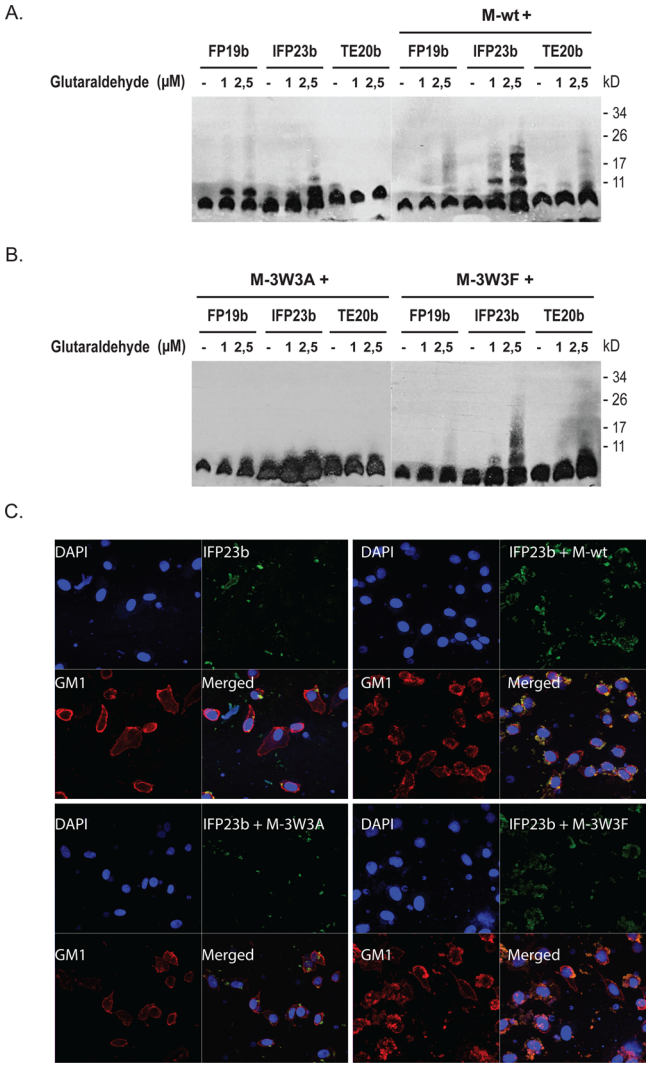

Figure 4. Formation of the M-wt−IFP23 heterohexamer and the participation of Trp residues in its interaction. (A) Formation of a heterohexamer by M-wt and IFP23b. M-wt (1 mM) was mixed with FP19b, IFP23b, or control peptide TE20b, at equimolar concentrations. Mixtures were incubated with 0, 1, or 2.5 mM glutaraldehyde at room temperature for 1 h and subjected to 16% Tricine SDS−PAGE and Western blotting using avidin-HRP. (B) Role of Trp residues in the formation of the M-wt−IFP23 heterohexamer. Peptide M-3W3A or M-3W3F (1 mM) was mixed with FP19b, IFP23b, or control peptide TE20b, at equimolar concentrations. The mixtures were incubated with 0, 1, or 2.5 mM glutaraldehyde at room temperature for 1 h and subjected to 16% Tricine SDS−PAGE and Western blotting using avidin-HRP. (C) M-wt allowed the translocation of IFP23b into the cell cytoplasm through the M-wt−IFP23 interaction. Vero E6 cells were treated with IFP23b or the M-wt/IFP23b, M-3W3A/IFP23b, or M-3W3F/IFP23b mixture for 30 min and subjected to immunofluorescence staining with Alex Fluor 594-conjugated CT-B (lipid raft marker GM1 staining, red), Dylight 488-conjugated Neutravidin (IPF-biotin staining, green), and DAPI (nuclear staining, purple).

retained in Vero cells (Figure 4C). However, in cells treated with the IFP23b/M-wt mixture, there was a substantial increase in the magnitude of the signal of IFP23b that was detected in the Vero cells (Figure 4C), with a pattern similar to those cells treated with biotinylated M-wt alone (Figure 2A). This result suggested an interaction between IFP23b and M-wt that enhanced the recruitment and retention of IFP23b to the Vero

DOI: 10.1021/bi501352u
Biochemistry 2015, 54, 1819−1830

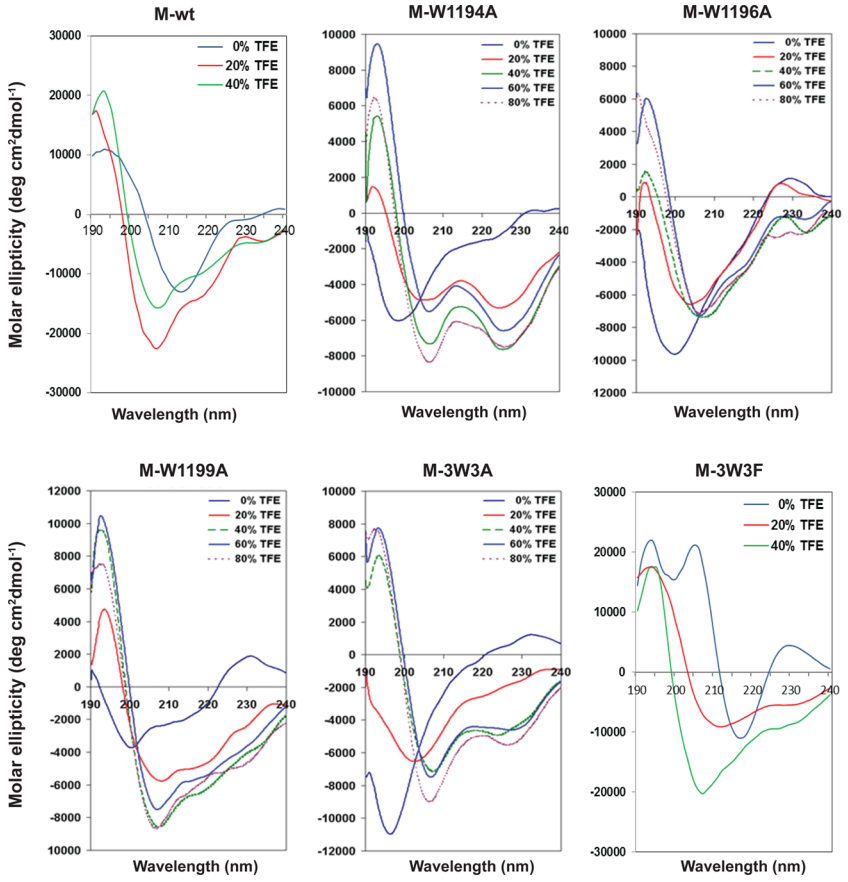

Figure 5. CD spectra of synthetic MPER peptides. M-wt, M-W1194A, M-W1196A, M-W1199A, or M-3W3A (1 mM each) was dissolved in H_2O supplemented with increasing concentrations of lipid mimetic TFE (0, 20, 40, 60, or 80%) and subjected to CD spectroscopy measurement at 25 °C. Secondary structure analyses were performed using CDNN.

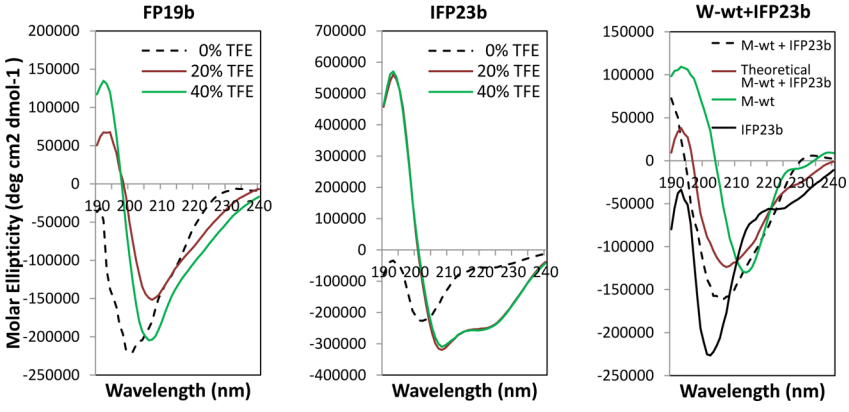

Figure 6. CD spectra of FP19b, IFP23b, and the M-wt/IFP23b mixture. FP19b adopted a β-sheet structure, while IFP23b adopted an increasingly α-helical structure when dissolved in lipidic solutions. FP19b or IFP23b (1 mM) was dissolved at increasing TFE concentrations (0, 20, or 40%) and subjected to CD spectroscopy measurement at 25 °C. Secondary structure analyses were performed using CDNN. The CD profile of the M-wt/IFP23b equimolar mixture (0.5 mM each) dissolved in ddH_2O was examined via CD spectroscopy and analyzed in a similar fashion.

cells. Consistent with our previous experiments, a similar IFP23b signal was observed in cells treated with the IFP23b/M-3W3A mixture or IFP23b alone, confirming the inability of IFP23b to bind to M-3W3A. In contrast, an increase in the magnitude of the IFP23b signal was observed in cells treated with the IFP23b/M-3W3F mixture, a level similar to that of the cells treated with the IFP23b/M-wt mixture, highlighting that M-3W3F recovered IFP23b binding ability. These results confirmed a potential interaction between MPER and IFP sequences that requires the participation of Trp residues in the MPER, in both the presence of cells and *in vitro* chemical cross-linking experiments.

Secondary Structure of MPER Peptides and the Contribution of Aromatic Residues to Their Structural Plasticity. MPER peptides in other class 1 viruses (e.g., HIV-1) have been known to adopt either β-strand or α-helical secondary structure under different biophysical conditions (e.g., solvent hydrophobicity).[32,33] Their structural plasticity raises

DOI: 10.1021/bi501352u
Biochemistry 2015, 54, 1819−1830

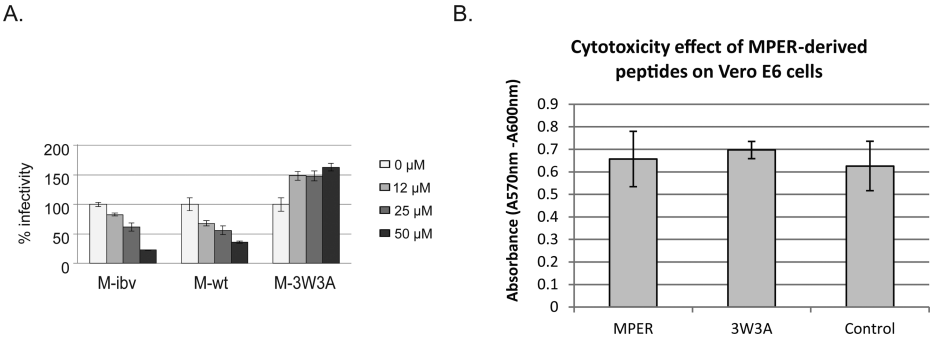

Figure 7. M-ibv and SARS-CoV M-wt inhibited IBV-Luc infection in Vero E6 cells. (A) IBV-Luc was mixed with increasing concentrations (0, 12.5, 25, and 50 μM) of M-ibv, M-wt, M-3W3A, or M-3W3F for 1 h at 37 °C and applied to Vero E6 cells at 1 PFU. Virus and peptides were removed 1 h postinfection. Cells were incubated at 37 °C for an additional 20 h, before being lysed and subjected to a luciferase assay. The percentage of infectivity was calculated on the basis of luciferase activity (n = 3; mean ± standard error). IC_{50} was calculated using GraphPad Prism. (B) Cytotoxicity effect of MPER-derived peptides tested on Vero E6 cells with PrestoBlue Cell Viability Reagent (Life Technologies), according to the manufacturer's protocol. Briefly, 50 μM M-wt, M-3W3A, or M-3W3F was incubated with 10000 Vero cells for 24 h. PrestoBlue cell viability reagent was subsequently added to the cells, and the absorbance at 570 and 600 nm was measured.

the possibility of the existence of more than one structure relevant to viral entry. To investigate the structural plasticity and its determining residues in the SARS-CoV MPER, CD spectroscopy was used to analyze the secondary structures of synthetic M-wt and its Ala- or Phe-substituted analogues. The MPER is in the proximity of the membrane, and the formation of the 6-HB in membrane fusion would further introduce an increasingly hydrophobic and lipidic environment around it. Indeed, MPER-derived peptides were capable of binding to cellular membranes, as demonstrated in the previous sections. To include the effect of the lipidic environment on MPER secondary structure, increasing concentrations of TFE, a lipid mimetic, were added to the solvent in this study. As shown in Figure 5, M-wt predominantly adopted a β-sheet structure under aqueous conditions, and an increase in TFE concentration to 40% prompted the peptide to adopt a more helical-like structure. M-3W3F bearing triple W → F substitutions exhibited a secondary structural profile similar to that of M-wt, under both aqueous and hydrophobic conditions (Figure 5).

Ala is a strong helix former, and the single-Ala-substituted analogues of Trp residues yielded contrasting results. Compared to M-wt, the two mutant peptides, M-W1196A and M-W1199A, exhibited similar structural changes in their CD profiles as solvent became increasingly hydrophobic. However, M-W1194A underwent a more abrupt structural change from a random-coil conformation in H_2O to typical α-helix (double minima at 208 and 222 nm) in 20% TFE; a conformational change persisted in 80% TFE. M-3W3A, containing triple Ala substitutions at all three Trp positions, adopted a structural change profile similar to that of M-W1194A (Figure 5).

Secondary Structure of FP, IFP, and the MPER/IFP Mixture. To study the conformational change of IFP and FP during fusion, the secondary structures of FP19b and IFP23b were assessed by CD spectroscopy at increasing TFE concentrations. The addition of 20% TFE, which increases solvent hydrophobicity, triggered IFP23b to adopt a primarily α-helical structure (Figure 6). In contrast, no substantial change was observed in FP19b with increasing TFE concentrations. The CD profile of M-wt and IFP23b as an equimolar mixture (0.5 mM each) differed from the theoretical CD profile averaged from the individual profiles of M-wtb and IFP23b, as the entire profile shifted 4 nm to the left, suggesting that there is a weak and transient interaction between M-wt and IFP23b in solution.

Inhibition of Virus Infectivity by Synthetic MPER Peptide and the Role of Trp. The ability of MPER in both complementary interaction (with IFP) and self-interaction raised the possibility that MPER-derived peptides could serve as viral entry inhibitors. In principle, both MPER and IFP are exposed during viral entry, and their association with a MPER-derived peptide could inhibit the progression of viral entry and infection. For safety reasons, the inhibitory activity of M-wt peptide was tested in neutralization assays using avian infectious bronchitis virus (IBV), instead of SARS-CoV. IBV contains the same MPER sequence and undergoes a fusion process synonymous to that of SARS-CoV. Specifically, the assay was conducted on recombinant IBV-Luc, which contains a firefly luciferase gene integrated at its ORF3a3b. Successful viral entry and subsequent replication of IBV-Luc were assessed by intracellular luciferase activity. The MPER peptide derived from IBV, M-ibv (LKTYIKWPWYVWLAIAF), was tested in parallel. Increasing concentrations of synthetic MPER peptides (0, 12, 25, and 50 μM) were mixed with IBV-Luc for 1 h at 37 °C and applied to Vero E6 cells seeded in a 96-well plate at 1 PFU. The peptide/virus mixture was removed 1 h post-infection. Cells were lysed 20 h postinfection, and luciferase activity was measured. As shown in Figure 7, M-ibv and M-wt inhibited IBV-Luc infection in a dose-dependent manner, with IC_{50} values of 29 and 26 μM, respectively. M-3W3A was also tested in parallel. M-3W3A completely lost its viral neutralization ability. The observed differential effect of M-wt (inhibition) and M-3W3A (no inhibition) on virus infectivity suggests the specific binding of synthetic M-wt to S protein is a key factor in its antiviral mechanisms.

To show that the MPER inhibition was not due to its toxicity effect, we determined its cytotoxicity on Vero E6 cells by the PrestoBlue assay. Peptides (50 μM) were incubated with Vero E6 cells for 24 h, before the cell viability was assayed. The viabilities of cells treated with 50 μM peptides are shown in Figure 7B. No statistical difference between viability of control (untreated) cells and treated cells was observed.

■ DISCUSSION

The MPER, a membrane-active region linking the external and transmembrane domains in S2 protein, is important for viral

DOI: 10.1021/bi501352u
Biochemistry 2015, 54, 1819−1830

infection as shown in previous mutational studies.[17] MPER sequences are highly conserved in *coronaviridae* and highly enriched with aromatic residues, particularly Trp. How do the Trp residues in MPER contribute to the viral entry and membrane fusion process and, in turn, infectivity? Using a panel of synthetic MPER peptides, this study showed that the Trp residues are important for MPER to interact with cellular membranes. More importantly, they played essential roles in maintaining structural plasticity, self-interaction of MPER-derived peptides, and inducing heterohexamer formation between MPER- and IFP-derived peptides during the viral entry process. In particular, the formation of the MPER−IFP complex provides insights after the formation of the 6-HB in the membrane fusion event.

Trp Residues in MPER Peptides Mediate Their Interaction with Membranes. Our study using Trp → Ala and Trp → Phe MPER analogues showed that Trp residues were essential for lipid mixing. This Trp-dependent effect was pronounced in the Trp → Ala analogues when the side-chain indole moiety of Trp was replaced by an alkyl moiety of Ala. In biological membranes, M-wt was found to be retained on Vero E6 cell membranes. In contrast, M-3W3A did not exhibit any binding to cell membranes. The phenotype was restored in the case of M-3W3F, where aromatic phenyl side chains were introduced back into the peptide. These data suggest that the aromatic side chains in MPER peptides are essential for maintaining their interaction with respect to attachment to biological membranes. Structural analysis by CD spectroscopy further demonstrated that a single Ala substitution (W1194A) or triple Ala substitutions (M-3W3A) resulted in these MPER analogues losing their structural plasticity and prematurely adopting a helical structure in a lipidic environment. Together with the previous mutational and biophysical studies, our data suggested that Trp residues in the S protein MPER are essential for membrane lipid mixing during membrane fusion and viral entry, possibly through maintaining a flexible MPER.[17,19]

Both Trp and Phe have aromatic side chains that are able to provide structural stability in a hydrophobic lipidic environment. However, the indole ring side chain of Trp potentiates a larger and more intense interaction through their π electrons, as compared to the phenyl side chain of Phe. The indole nitrogen of Trp could function as a weak base and hydrogen bond donor, leading to hydrogen bonds formed with the lipid headgroups.[34] This could lead to the differential membrane partitioning ability of Trp and Phe, when they are placed at juxtamembrane positions.[35] Whereas Trp prefers the interfacial position and serves as a "buoy" to adjacent transmembrane domain, because of its balanced attraction toward and repulsion from the membrane, Phe is sufficiently hydrophobic to sink into and reside in the hydrophobic core of the lipid bilayer with the transmembrane segment.[18,34,36−38] The subtle difference between Trp and Phe might have disorganized the orchestrated fusion process and contributed to a substantial loss of viral infectivity when a single W → F substitution at a critical position (e.g., W1194) was introduced into the MPER of the pseudotyped SARS-CoV,[19] although the M-3W3F and M-wt peptides differed little in structural plasticity and membrane binding capability.

MPER-Derived Peptides Self-Oligomerized and Formed a Heterohexamer with the IFP-Derived Peptide. In the prefusion state, S proteins exist as trimers through self-interactions between domains on neighboring proteins, such as HR2. To examine if MPER could exist as a structural extender of trimerized HR2 in the prefusion stage, we investigated the oligomerization ability of MPER-derived peptides. Ala and Phe analogues were examined in parallel to reveal the participation of Trp in this process. Interactions between shorter peptides tend to be weak and unstable, a persistent challenge in the deconstruction approach using peptides to examine protein−protein interactions. The potential interaction between MPERs was stabilized and observed through the chemical cross-linker glutaraldehyde, which captures transient interactions as covalent complexes. The M-wt peptide produced dimer, trimer, and high-molecular weight oligomers starting from 1 mM glutaraldehyde. No trimer or high-order oligomers were detected in the triple-Ala mutant M-3W3A, whereas the single-Ala substitution at W1194, W1196, and W1199 did not significantly affect the oligomerization. Together, these data suggested that M-wt oligomerization is maintained by multiple aromatic amino acids, and the loss of aromaticity at a single position is insufficient to disrupt oligomerization.

A possible motif that could explain the requirement of aromatic residues in maintaining MPER−MPER interaction is an aromatic amino acid zipper (AAAZ). The zipper motifs have previously been proposed to exist among aromatic amino acids, including Trp, Phe, and Tyr, to stabilize peptide or protein structures and induce oligomerization.[39] Engineered cross-strand Trp-Trp pairs were shown to induce stable β-hairpin peptides, where the indole ring side chains of Trp residues were stacked perpendicularly forming a "Trp zipper".[40] Subsequently, the "Trp zipper" motif was either discovered in or introduced into proteins to stabilize protein quaternary structure.[41,42] Potentially, the oligomerization of MPER peptides could be facilitated by the hydrophobic interaction (e.g., $\pi-\pi$ interaction) between aromatic residues on the neighboring peptide. The interdigitating stacking of their aromatic ring side chains would generate a zipperlike motif, or AAAZ motif, to facilitate peptide−peptide interaction. Thus, removing aromatic side chains by Ala substitution of W1194, W1196, and W1199 deters AAAZ formation. In contrast, substitutions of Trp with Phe, another aromatic amino acid, could maintain the AAAZ motif and hence peptide oligomerization. Furthermore, the AAAZ motif is likely sustained by multiple aromatic amino acids, and the loss of one aromatic amino acid at a single position would unlikely disrupt the motif, as shown by our mutational study with a single Trp → Ala substitution.

As viral entry begins, the HR2 trimer dissociates and folds back onto the central HR1 as a coiled-coil 6-HB through complementary binding. Upon the formation of the 6-HB, hydrophobic and membrane-active segments upstream of HR1 (e.g., FP and IFP) and the segments downstream of HR2 (e.g., MPER and TM) come into the proximity of each other, potentiating their interactions. Two groups have used protein engineering to construct a part or the entire ectodomain of gp41 HIV containing HR1 and/or HR2. They showed that the FPPR (fusion peptide proximal region) and MPER come together as continuous helices, extending the trimer-of-trimer structure of the 6-HB.[43,44] The FPPR of gp41 HIV is the equivalent of the IFP of SARS-CoV. In our study, cross-linking experiments stabilized and revealed a peptide−peptide interaction between synthetic peptides M-wt and IFP23b, but not between M-wt and FP19b. An advantage of using glutaraldehyde is that the cross-linking reaction is generally mediated by the formation of an imine with the N-terminal amines. As such, the self-interaction of M-wt or IFP23b is likely

DOI: 10.1021/bi501352u
Biochemistry 2015, 54, 1819−1830

through their N-terminal amines and occurs in parallel fashion.[43] This weak and transient interaction between M-wt and IFP23b was further observed in the CD spectra as the equimolar mixture adopted a new secondary structural profile (Figure 6).

The putative MPER−IFP interaction was further confirmed under a physiologically relevant condition, as the peptides were co-applied to Vero E6 cells and examined through immunofluorescence staining. Indeed, more IFP23b was recruited to and retained on the cell membrane, upon the addition of M-wt. We concluded that the membrane-active M-wt bound to the Vero E6 cell membrane and interacted with IFP23b, indirectly enhancing the retention of IFP23b. The ability of MPER to bind and recruit IFP to the cell membrane lipid without membrane lysis may be of interest in drug design (see Results in using the MPER as inhibitor).

Amino acids W1194, W1196, and W1199 are also involved in M-wt−IFP23 heterohexamer formation. Chemical cross-linking and immunofluorescence staining showed that triple Ala substitution of Trp in M-wt abolishes M-wt−IFP23 interaction, which is partially recovered by Ala → Phe substitution. The putative interaction between MPER and IFP may serve as a continuum of a quaternary protein structure to the 6-HB in providing membrane-interacting surfaces and a low-energy barrier path for lipid flow and membrane fusion. Unlike the Leu/Ile zipper of HR1 and HR2, the sequence mediating MPER−IFP interaction is short and the interaction is unlikely to be stable.

Structural Flexibility of the MPER and IFP and the Role of Three Trp Residues. In agreement with studies by others, we showed that the synthetic MPER and IFP derived from SARS-CoV S protein are structurally flexible. They transit from a predominantly β-strand conformation to α-helix in a lipidic environmental lipid. The MPER may undergo conformational changes, undergoing a transition from a β-sheet conformation in its prefusion state when it is solvent-exposed to a helical structure in its postfusion state that is solvent-shielded and a more hydrophobic environment in the presence of membrane lipids. Similarly, the structural flexibility of MPER peptides was also observed in HIV gp41, Ebola virus GP2, and influenza virus HA protein and is believed to be essential for the conformational transition of fusion proteins.[21,23,27,28]

A structural basis for the structural flexibility of SARS-CoV S protein in our MPER peptides may be their N-terminal sequence (KYEQYIK), which is composed of alternating hydrophobic and hydrophilic residues. Such residues constitute a motif favoring β-strand formation. Previous studies have shown that hydrophilic residues (K1187, E1189, and K1193) with a motif of alternating charge distribution (+ − +) can adopt a helix or β-strand arrangement after environmental changes (e.g., pH or hydrophobicity changes).[45] The observed hydrophobicity-triggered β-strand to α-helix structural transition for MPER is likely attributed to its flexible N-terminus. The C-terminus (WPWYVWLGF) of MPER is composed of eight hydrophobic residues, five of which are aromatic amino acids (W1194, W1196, Y1197, W1199, and F1202). Under aqueous conditions, the bulky aromatic residues, especially W1194, of the C-terminus of the MPER serve as a helix breaker, constraining the peptide into a β-sheet conformation.

Of the three Trp residues in the MPER, W1194 appears to play a role more important than that of W1196 and W1199 in maintaining structural flexibility. Substituting W1194 with Ala forced the synthetic MPER analogue to prematurely adopt helical structure in a lipidic environment. W1194 is the Trp residue adjoining the KYEQYIK segment and Ala is a strong helix former. This combination likely facilitates the α-helical formation of M-W119A. Thus, Trp → Ala substitution may force MPER prematurely to adopt a helical structure, hampering proper conformational change and subsequently preventing the putative quaternary intermediate formation. Loss of infectivity of virus pseudotyped with S mutants (substitutions of Trp with Ala in the MPER) may be attributed to this explanation.[19]

Synthetic MPER Peptide as a Virus Entry Inhibitor. The MPER has been reported to be an exposed region harboring epitopes for broadly neutralizing antibodies and regarded as a desirable target for antiviral therapeutics for its accessibility and sequential conservation.[46−51] Indeed, the inclusion of MPER sequences has been proven to be essential for both first- and second-generation fusion inhibitors against HIV-1. Similarly, an octapeptide derived from the FIV MPER has been shown to act as a mild entry inhibitor.[52,53] In virus inhibition assays, both peptides derived from IBV M-ibv and SARS-CoV M-wt inhibited IBV-Luc entry and infection. M-3W3A totally loses its virus neutralization ability. M-wt peptide may play multiple roles when applied to both the virus and human cells. It may bind to S2, interfering with its conformational change, and perturbs cell membrane integrity to facilitate fusion or to reduce viral viability.

CONCLUSION

In conclusion, our study of the SARS-CoV MPER agrees with our previous work on the MPER and those on class I virus fusion glycoproteins (e.g., HIV and EboV). The dominant factor in maintaining diverse roles of the MPER is its Trp-rich motif, which allows it to self-bind, form a high-order complex with IFP, and perform a membrane mixing function. The synthetic MPER showed antiviral activity and has an added advantage in its water solubility compared to fusion peptides, a useful feature for developing a bioactive peptide as a fusion inhibitor.

AUTHOR INFORMATION

Corresponding Author

*E-mail: jptam@ntu.edu.sg. Telephone: (65)63162822. Fax: (65)67913856.

Author Contributions

Y.L. and S.M.Z. contributed equally to this work.

Funding

This research was supported by a Competitive Research Grant from the National Research Foundation of Singapore (NRF-CRP8-2011-05).

Notes

The authors declare no competing financial interest.

ABBREVIATIONS

CoV, coronavirus; SARS, severe acute respiratory syndrome; S protein, spike protein; MPER, membrane proximal external region; FP, fusion peptide; HR, heptad repeat; TM, transmembrane domain; IBV, Aavian infectious bronchitis virus; HIV-1, human immunodeficiency virus type 1; FIV, feline immunodeficiency virus; CD, circular dichroism; DMEM, Dulbecco's modified Eagle's medium; AAAZ, aromatic amino acid zipper.

DOI: 10.1021/bi501352u
Biochemistry 2015, 54, 1819−1830

REFERENCES

(1) Ksiazek, T. G., Erdman, D., Goldsmith, C. S., Zaki, S. R., Peret, T., Emery, S., Tong, S., Urbani, C., Comer, J. A., Lim, W., Rollin, P. E., Dowell, S. F., Ling, A. E., Humphrey, C. D., Shieh, W. J., Guarner, J., Paddock, C. D., Rota, P., Fields, B., DeRisi, J., Yang, J. Y., Cox, N., Hughes, J. M., LeDuc, J. W., Bellini, W. J., and Anderson, L. J. (2003) A novel coronavirus associated with severe acute respiratory syndrome. *N. Engl. J. Med. 348*, 1953−1966.

(2) Peiris, J. S., Lai, S. T., Poon, L. L., Guan, Y., Yam, L. Y., Lim, W., Nicholls, J., Yee, W. K., Yan, W. W., Cheung, M. T., Cheng, V. C., Chan, K. H., Tsang, D. N., Yung, R. W., Ng, T. K., and Yuen, K. Y. (2003) Coronavirus as a possible cause of severe acute respiratory syndrome. *Lancet 361*, 1319−1325.

(3) Rota, P. A., Oberste, M. S., Monroe, S. S., Nix, W. A., Campagnoli, R., Icenogle, J. P., Penaranda, S., Bankamp, B., Maher, K., Chen, M. H., Tong, S., Tamin, A., Lowe, L., Frace, M., DeRisi, J. L., Chen, Q., Wang, D., Erdman, D. D., Peret, T. C., Burns, C., Ksiazek, T. G., Rollin, P. E., Sanchez, A., Liffick, S., Holloway, B., Limor, J., McCaustland, K., Olsen-Rasmussen, M., Fouchier, R., Gunther, S., Osterhaus, A. D., Drosten, C., Pallansch, M. A., Anderson, L. J., and Bellini, W. J. (2003) Characterization of a novel coronavirus associated with severe acute respiratory syndrome. *Science 300*, 1394−1399.

(4) Simmons, G., Gosalia, D. N., Rennekamp, A. J., Reeves, J. D., Diamond, S. L., and Bates, P. (2005) Inhibitors of cathepsin L prevent severe acute respiratory syndrome coronavirus entry. *Proc. Natl. Acad. Sci. U.S.A. 102*, 11876−11881.

(5) Bosch, B. J., Bartelink, W., and Rottier, P. J. (2008) Cathepsin L functionally cleaves the severe acute respiratory syndrome coronavirus class I fusion protein upstream of rather than adjacent to the fusion peptide. *J. Virol. 82*, 8887−8890.

(6) Li, W., Moore, M. J., Vasilieva, N., Sui, J., Wong, S. K., Berne, M. A., Somasundaran, M., Sullivan, J. L., Luzuriaga, K., Greenough, T. C., Choe, H., and Farzan, M. (2003) Angiotensin-converting enzyme 2 is a functional receptor for the SARS coronavirus. *Nature 426*, 450−454.

(7) Liu, S., Xiao, G., Chen, Y., He, Y., Niu, J., Escalante, C. R., Xiong, H., Farmar, J., Debnath, A. K., Tien, P., and Jiang, S. (2004) Interaction between heptad repeat 1 and 2 regions in spike protein of SARS-associated coronavirus: Implications for virus fusogenic mechanism and identification of fusion inhibitors. *Lancet 363*, 938−947.

(8) Tripet, B., Howard, M. W., Jobling, M., Holmes, R. K., Holmes, K. V., and Hodges, R. S. (2004) Structural characterization of the SARS-coronavirus spike S fusion protein core. *J. Biol. Chem. 279*, 20836−20849.

(9) Guillen, J., de Almeida, R. F., Prieto, M., and Villalain, J. (2008) Structural and dynamic characterization of the interaction of the putative fusion peptide of the S2 SARS-CoV virus protein with lipid membranes. *J. Phys. Chem. B 112*, 6997−7007.

(10) Guillen, J., Kinnunen, P. K., and Villalain, J. (2008) Membrane insertion of the three main membranotropic sequences from SARS-CoV S2 glycoprotein. *Biochim. Biophys. Acta 1778*, 2765−2774.

(11) Guillen, J., Perez-Berna, A. J., Moreno, M. R., and Villalain, J. (2005) Identification of the membrane-active regions of the severe acute respiratory syndrome coronavirus spike membrane glycoprotein using a 16/18-mer peptide scan: Implications for the viral fusion mechanism. *J. Virol. 79*, 1743−1752.

(12) Guillen, J., Perez-Berna, A. J., Moreno, M. R., and Villalain, J. (2008) A second SARS-CoV S2 glycoprotein internal membrane-active peptide. Biophysical characterization and membrane interaction. *Biochemistry 47*, 8214−8224.

(13) Park, H. E., Gruenke, J. A., and White, J. M. (2003) Leash in the groove mechanism of membrane fusion. *Nat. Struct. Biol. 10*, 1048−1053.

(14) Chu, L. H., Chan, S. H., Tsai, S. N., Wang, Y., Cheng, C. H., Wong, K. B., Waye, M. M., and Ngai, S. M. (2008) Fusion core structure of the severe acute respiratory syndrome coronavirus (SARS-CoV): In search of potent SARS-CoV entry inhibitors. *J. Cell. Biochem. 104*, 2335−2347.

(15) Petit, C. M., Melancon, J. M., Chouljenko, V. N., Colgrove, R., Farzan, M., Knipe, D. M., and Kousoulas, K. G. (2005) Genetic analysis of the SARS-coronavirus spike glycoprotein functional domains involved in cell-surface expression and cell-to-cell fusion. *Virology 341*, 215−230.

(16) Sainz, B., Jr., Rausch, J. M., Gallaher, W. R., Garry, R. F., and Wimley, W. C. (2005) Identification and characterization of the putative fusion peptide of the severe acute respiratory syndrome-associated coronavirus spike protein. *J. Virol. 79*, 7195−7206.

(17) Sainz, B., Jr., Rausch, J. M., Gallaher, W. R., Garry, R. F., and Wimley, W. C. (2005) The aromatic domain of the coronavirus class I viral fusion protein induces membrane permeabilization: Putative role during viral entry. *Biochemistry 44*, 947−958.

(18) Corver, J., Broer, R., van Kasteren, P., and Spaan, W. (2009) Mutagenesis of the transmembrane domain of the SARS coronavirus spike glycoprotein: Refinement of the requirements for SARS coronavirus cell entry. *Virol. J. 6*, 230.

(19) Lu, Y., Neo, T. L., Liu, D. X., and Tam, J. P. (2008) Importance of SARS-CoV spike protein Trp-rich region in viral infectivity. *Biochem. Biophys. Res. Commun. 371*, 356−360.

(20) Howard, M. W., Travanty, E. A., Jeffers, S. A., Smith, M. K., Wennier, S. T., Thackray, L. B., and Holmes, K. V. (2008) Aromatic amino acids in the juxtamembrane domain of severe acute respiratory syndrome coronavirus spike glycoprotein are important for receptor-dependent virus entry and cell-cell fusion. *J. Virol. 82*, 2883−2894.

(21) Salzwedel, K., West, J. T., and Hunter, E. (1999) A conserved tryptophan-rich motif in the membrane-proximal region of the human immunodeficiency virus type 1 gp41 ectodomain is important for Env-mediated fusion and virus infectivity. *J. Virol. 73*, 2469−2480.

(22) Giannecchini, S., Bonci, F., Pistello, M., Matteucci, D., Sichi, O., Rovero, P., and Bendinelli, M. (2004) The membrane-proximal tryptophan-rich region in the transmembrane glycoprotein ectodomain of feline immunodeficiency virus is important for cell entry. *Virology 320*, 156−166.

(23) Bullough, P. A., Hughson, F. M., Skehel, J. J., and Wiley, D. C. (1994) Structure of influenza haemagglutinin at the pH of membrane fusion. *Nature 371*, 37−43.

(24) Saez-Cirion, A., Gomara, M. J., Agirre, A., and Nieva, J. L. (2003) Pre-transmembrane sequence of Ebola glycoprotein. Interfacial hydrophobicity distribution and interaction with membranes. *FEBS Lett. 533*, 47−53.

(25) Vishwanathan, S. A., and Hunter, E. (2008) Importance of the membrane-perturbing properties of the membrane-proximal external region of human immunodeficiency virus type 1 gp41 to viral fusion. *J. Virol. 82*, 5118−5126.

(26) Suarez, T., Gallaher, W. R., Agirre, A., Goni, F. M., and Nieva, J. L. (2000) Membrane interface-interacting sequences within the ectodomain of the human immunodeficiency virus type 1 envelope glycoprotein: Putative role during viral fusion. *J. Virol. 74*, 8038−8047.

(27) Weissenhorn, W., Dessen, A., Harrison, S. C., Skehel, J. J., and Wiley, D. C. (1997) Atomic structure of the ectodomain from HIV-1 gp41. *Nature 387*, 426−430.

(28) Regula, L. K., Harris, R., Wang, F., Higgins, C. D., Koellhoffer, J. F., Zhao, Y., Chandran, K., Gao, J., Girvin, M. E., and Lai, J. R. (2013) Conformational Properties of Peptides Corresponding to the Ebolavirus GP2Membrane-Proximal External Region in the Presence of Micelle-Forming Surfactants and Lipids. *Biochemistry 52*, 3393−3404.

(29) Akkarawongsa, R., Pocaro, N. E., Case, G., Kolb, A. W., and Brandt, C. R. (2009) Multiple peptides homologous to herpes simplex virus type 1 glycoprotein B inhibit viral infection. *Antimicrob. Agents Chemother. 53*, 987−996.

(30) Schagger, H. (2006) Tricine-SDS-PAGE. *Nat. Protoc. 1*, 16−22.

(31) Li, H., and Papadopoulos, V. (1998) Peripheral-type benzodiazepine receptor function in cholesterol transport. Identification of a putative cholesterol recognition/interaction amino acid sequence and consensus pattern. *Endocrinology 139*, 4991−4997.

(32) Schibli, D. J., Montelaro, R. C., and Vogel, H. J. (2001) The membrane-proximal tryptophan-rich region of the HIV glycoprotein,

DOI: 10.1021/bi501352u
Biochemistry 2015, 54, 1819−1830

gp41, forms a well-defined helix in dodecylphosphocholine micelles. *Biochemistry 40*, 9570−9578.
(33) Ofek, G., Tang, M., Sambor, A., Katinger, H., Mascola, J. R., Wyatt, R., and Kwong, P. D. (2004) Structure and mechanistic analysis of the anti-human immunodeficiency virus type 1 antibody 2F5 in complex with its gp41 epitope. *J. Virol. 78*, 10724−10737.
(34) Dougherty, D. A. (1996) Cation-π interactions in chemistry and biology: A new view of benzene, Phe, Tyr, and Trp. *Science 271*, 163−168.
(35) Yau, W. M., Wimley, W. C., Gawrisch, K., and White, S. H. (1998) The preference of tryptophan for membrane interfaces. *Biochemistry 37*, 14713−14718.
(36) Braun, P., and von Heijne, G. (1999) The aromatic residues Trp and Phe have different effects on the positioning of a transmembrane helix in the microsomal membrane. *Biochemistry 38*, 9778−9782.
(37) Killian, J. A., and von Heijne, G. (2000) How proteins adapt to a membrane-water interface. *Trends Biochem. Sci. 25*, 429−434.
(38) van Duyl, B. Y., Meeldijk, H., Verkleij, A. J., Rijkers, D. T., Chupin, V., de Kruijff, B., and Killian, J. A. (2005) A synergistic effect between cholesterol and tryptophan-flanked transmembrane helices modulates membrane curvature. *Biochemistry 44*, 4526−4532.
(39) Liu, J., Zheng, Q., Deng, Y., Kallenbach, N. R., and Lu, M. (2006) Conformational transition between four and five-stranded phenylalanine zippers determined by a local packing interaction. *J. Mol. Biol. 361*, 168−179.
(40) Cochran, A. G., Skelton, N. J., and Starovasnik, M. A. (2001) Tryptophan zippers: Stable, monomeric β-hairpins. *Proc. Natl. Acad. Sci. U.S.A. 98*, 5578−5583.
(41) Liu, J., Yong, W., Deng, Y., Kallenbach, N. R., and Lu, M. (2004) Atomic structure of a tryptophan-zipper pentamer. *Proc. Natl. Acad. Sci. U.S.A. 101*, 16156−16161.
(42) Jager, M., Dendle, M., Fuller, A. A., and Kelly, J. W. (2007) A cross-strand Trp-Trp pair stabilizes the hPin1 WW domain at the expense of function. *Protein Sci. 16*, 2306−2313.
(43) Buzon, V., Natrajan, G., Schibli, D., Campelo, F., Kozlov, M. M., and Weissenhorn, W. (2010) Crystal structure of HIV-1 gp41 including both fusion peptide and membrane proximal external regions. *PLoS Pathog. 6*, e1000880.
(44) Bellamy-McIntyre, A. K., Lay, C. S., Baar, S., Maerz, A. L., Talbo, G. H., Drummer, H. E., and Poumbourios, P. (2007) Functional links between the fusion peptide-proximal polar segment and membrane-proximal region of human immunodeficiency virus gp41 in distinct phases of membrane fusion. *J. Biol. Chem. 282*, 23104−23116.
(45) Zhang, S., Lockshin, C., Herbert, A., Winter, E., and Rich, A. (1992) Zuotin, a putative Z-DNA binding protein in *Saccharomyces cerevisiae*. *EMBO J. 11*, 3787−3796.
(46) Dimitrov, A. S., Jacobs, A., Finnegan, C. M., Stiegler, G., Katinger, H., and Blumenthal, R. (2007) Exposure of the membrane-proximal external region of HIV-1 gp41 in the course of HIV-1 envelope glycoprotein-mediated fusion. *Biochemistry 46*, 1398−1401.
(47) Sattentau, Q. J., Zolla-Pazner, S., and Poignard, P. (1995) Epitope exposure on functional, oligomeric HIV-1 gp41 molecules. *Virology 206*, 713−717.
(48) Finnegan, C. M., Berg, W., Lewis, G. K., and DeVico, A. L. (2002) Antigenic properties of the human immunodeficiency virus transmembrane glycoprotein during cell-cell fusion. *J. Virol. 76*, 12123−12134.
(49) Purtscher, M., Trkola, A., Gruber, G., Buchacher, A., Predl, R., Steindl, F., Tauer, C., Berger, R., Barrett, N., Jungbauer, A., et al. (1994) A broadly neutralizing human monoclonal antibody against gp41 of human immunodeficiency virus type 1. *AIDS Res. Hum. Retroviruses 10*, 1651−1658.
(50) Zwick, M. B., Labrijn, A. F., Wang, M., Spenlehauer, C., Saphire, E. O., Binley, J. M., Moore, J. P., Stiegler, G., Katinger, H., Burton, D. R., and Parren, P. W. (2001) Broadly neutralizing antibodies targeted to the membrane-proximal external region of human immunodeficiency virus type 1 glycoprotein gp41. *J. Virol. 75*, 10892−10905.
(51) Lorizate, M., Cruz, A., Huarte, N., Kunert, R., Perez-Gil, J., and Nieva, J. L. (2006) Recognition and blocking of HIV-1 gp41 pre-transmembrane sequence by monoclonal 4E10 antibody in a raft-like membrane environment. *J. Biol. Chem. 281*, 39598−39606.
(52) Freer, G., Giannecchini, S., Tissot, A., Bachmann, M. F., Rovero, P., Serres, P. F., and Bendinelli, M. (2004) Dissection of seroreactivity against the tryptophan-rich motif of the feline immunodeficiency virus transmembrane glycoprotein. *Virology 322*, 360−369.
(53) Giannecchini, S., Alcaro, M. C., Isola, P., Sichi, O., Pistello, M., Papini, A. M., Rovero, P., and Bendinelli, M. (2005) Feline immunodeficiency virus plasma load reduction by a retroinverso octapeptide reproducing the Trp-rich motif of the transmembrane glycoprotein. *Antiviral Ther. 10*, 671−680.

DOI: 10.1021/bi501352u
Biochemistry 2015, 54, 1819−1830